PCCP

Accepted Manuscript

ROYAL SOCIETY OF CHEMISTRY

www.rsc.org/pccp

Physical Chemistry Chemical Physics
CREATED USING THE RSC LaTeX PCCP ARTICLE TEMPLATE – SEE www.rsc.org/electronicfiles FOR DETAILS
ARTICLE TYPE www. rsc.org/xxxxxx | XXXXXXXX

Kinetics of aggregation in liquids with dispersed nanoparticles

Wojciech Jeżewski[a]

Received Xth XXXXXXXXXX 20XX, Accepted Xth XXXXXXXXX 20XX
First published on the web Xth XXXXXXXXXX 200X
DOI: 10.1039/b000000x

The process of attaching molecules of liquid media by dispersed nanoparticles is modeled and numerically studied. The growth rate of the resulting nanoparticle-induced aggregates is determined by assuming the preferential attachment rule according to which the effectiveness of the connection of a new molecular unit to aggregates is determined by their size. It is shown that, depending on a specific function form of the growing rate, the size distribution of aggregates can display very different shapes, including various multimodal structures. This can explain experimentally obtained complex size distributions of inhomogeneous aggregates appearing in consequence of the adsorption of molecules by nanoparticles or in consequence of the self-assembling of active dispersant on surfaces of nanoparticles. The time evolution and the stationarity of the size distribution are also analyzed, yielding an insight into the long-time behavior of systems with dispersed nanoparticles.

1 Introduction

The immersion of nanoparticles (NPs) in various liquid media, especially in reactive solvents, is an effective approach to prepare composite materials with controllable properties.[1,2] Since NP inclusions cause, in general, metastability of the resulting mixtures, the dispersed NPs reveal a strong tendency to reduce the free energy of the mixtures through the processes of segregation, aggregation, agglomeration, nucleation, or crystallization.[3–15] Another possibility to minimize the free energy is asociated with attaching molecules or molecular blocks of liquid media by the NPs.[16–19] Superparticles appearing as a consequence of such aggregation, can have very different sizes and can display very various forms, in particular dendric and compact core-shell shapes.[16–18,20,21] The superparticles can also exhibit an ability to form organized structures with diversified morphologies. Then, the process of organization runs at different spatial scales giving the opportunity to construct, in a controllable manner, complex materials that display appropriate functional properties on different structural levels.[22] An opposite, in some sense, motivation to study the process of aggregation is associated with cases for which this process is unfavorable.[23]

Perhaps the most basic and important characteristics of the structural inhomogeneity of NP systems can be obtained by investigating the size distribution (SD) of NPs or NP-induced superparticles. This distribution can experimentally be determined using the static and dynamic light scattering methods,[20,23] the NP tracking analysis,[24] the small-angle X-ray scattering technique,[25] the scanning microscopy,[15] the transmission electron microscopy,[26] etc. Whereas the time variation of SD reflects the process of organization of NP systems, including the formation of NP crystals,[5,7] the long-time behavior of SD characterizes the steady state of these systems. Depending on specific features of NP systems, the SD of dispersed NPs have been shown to display not only different time evolutions but also a wide diversity of long-time behaviors. Clearly, in cases of homogeneous (monodispersive) or nearly homogeneous NP systems, the SD exhibits a very narrow single-peaked form. Nearly homogeneous SDs have been found, e.g., for systems produced during sintering of primary aggregates,[12,27] for systems of thermally-reencapsulated core-shell nanoparticles,[28] and for large nanocrystals formed through the aggregation and coalescence of small primary nanocrystals.[5] Typical SDs in inhomogeneous NP systems have been shown to be well described by single-peaked functions of different forms, ranging from relatively narrow to distinctly broad, usually skewed in the right direction.[26] In general, the significantly skewed unimodal SDs can be expected to occur when the organization of NP ensembles proceeds in a complex or multistage (hierarchical) manner. Indeed, such asymmetric distributions have experimentally been determined, e.g., for systems organized through the competition between capping and reducing agents,[25] as well as for systems of aggregates appeared as a result of the incorporation of water,[29] or in consequence of a two-stage process of the attachment of monomers to NPs and the aggregation of the resulting NPs.[7] It should also be noted that the exponential form of the SD of aggregates can arise when there is no interaction between aggregates or when the interactions are very weak.[29,30] Undoubtedly, the most intriguing SDs are those re-

[a] *Institute of Molecular Physics, Polish Academy of Sciences, Smoluchowskiego 17, Poznań, Poland.*
E-mail: jezewski@ifmpan.poznan.pl

† Electronic Supplementary Information (ESI) available: [details of any supplementary information available should be included here]. See DOI: 10.1039/b000000x/

vealing multimodal shapes. The multimodal SDs have been derived for aggregate systems that are organized in a strongly heterogeneous way, due to, e.g., the adhesion of particles of specific sizes to substrates, or due to the connection of particles to particles of other kinds. [18,20,24]

To develop the theoretical analysis of the formation of NP systems, one can essentially exploit some of the formalisms already introduced in studying processes of coalescence, coagulation, or fragmentation of molecules. For instance, the aggregation process of NPs can be investigated using the approach based on the kinetic coagulation Smoluchowski equation, or on its modified or extended versions. [31–37] It has been argued that this equation accurately describe the aggregation of clusters with the fractal structure. [31] The resulting SD has been shown to exhibit self-similarity for both constant aggregation rates (related to the diffusion limited aggregation) and some homogeneous aggregation rates. [34,35] Numerical modeling and simulations of cluster and/or NP systems have mainly been concentrated on investigating the process of formation of fractal aggregates (taking into account the time evolution of their shapes and SDs) as well as on investigating the effect of pair interactions between particles on the aggregation process. [13,38–43] It is remarkable that both analytical and numerical approaches to analyze the evolution of NP ensembles often refer to systems in which the maximal number of agglomerates changes in time and is not strictly specified or even unconfined. However, such systems are rather unrealistic, although the number of NPs contained in real systems can fluctuate in time.

In this paper, a model of complex systems in which dispersed NPs can attach molecules constituting fluid media, but in which the NPs and greater particles (aggregates) do not joint together, is considered. Consequently, within this model, the number of the particles is independent of time. Despite the model does not concern the formation of links between preformed NPs, it can be applied to describe kinetics of a large variety of real NP systems. These systems include ensembles in which the contact and the connection between NPs are prevented due to repulsive interaction, [13,20] or due to coating NPs by molecules of fluid media. Depending on the context, the coated NPs are also referred to as encapsulated particles, [44] NPs surface-capped by agents in reactive environments, [5,25,45] core-shell NPs [18,19,46] or core-shell micelles. [18,46,47] An analogous complex structures have also been argued to occur in liquid crystal systems in which molecules with hydrophilic side chains are attracted by small dispersed water droplets. [16] The coating process can lead to the appearance of very large aggregate objects with complex molecular groups anchored to surfaces of NPs. The attached molecular groups can exhibit different sizes and spatial conformations, such as linear long chains, unbranched polymers, and branched polymers (dendrimers). [17–19,45,48] Obviously, the resulting complex ensembles can be strongly inhomogeneous with respect to total sizes of aggregate objects. Then, the time evolution of individual aggregates proceeds with different attachment rates, dependent on the actual size of aggregates and on the current shape of their surfaces. To take into consideration the possibility of forming inhomogeneous NP-induced ensembles within the introduced model, the aggregation rate is treated as a function of the size of individual aggregates.

2 Theoretical model and calculation procedure

In systems of NPs suspended in fluid media, the particles can, in general, attach other particles and/or molecules of the media. Here, the case when the formation of any connections between the preformed NPs is not allowed, in consequence, e.g., of the electrostatic repulsion is considered. Similarly, the merging of agglomerates created by attaching molecules of media to NPs is also prevented. Thus, within the studied model system, dispersed preexisting NPs play a role of seeds that absorb molecules of the dispersion phase, stabilizing and functionalizing resulting greater particles (aggregates). Alternatively, the model concerns systems in which reactive molecules of media or surface-active dispersants self-assemble on NP surface forming dense polymer layers or more complex structures with functionalities for targeting. [18] Both the processes of adsorption and self-assembling on surface of NPs are allowed here to lead to the formation of polydispersive ensemble of noninteracting particles. Consequently, within this model, the number, say n, of preformed NPs is constant and, at each stage of the time evolution of the system, is equal to the total number of possible aggregates and NPs that have not yet attached any molecule. Moreover, it is assumed that the overall concentrations of the preformed NPs and aggregates are low enough, so correlations between local aggregation processes can be ignored. Although sizes of the preformed NPs can in general be different, the size of each of the agglomerates is expressed here by the number of their component parts. Thus, the size of the ith, $i = 1,2,...,n$, agglomerate is given by $s_i = s'_i + 1$, where $s'_i \geqslant 0$ is the number of the molecules connected to the ith NP. Since, the pure (unconnected) NPs are treated here as agglomerates of the size $s = 1$, the agglomerates and pure NPs are henceforth referred to as particles. Then, the number n of the preformed NPs is equal to the number of particles.

The attaching rate of a new molecule to particle i is postulated to depend on the size s_i of the particle i. This assumption reflects the supposition that the attachment rate is determined by the shape and the surface area of a given particle as well as by the strength of interactions between particles and molecules. [4,11,13,45] Consequently, the effective rate

of connecting a molecule to ith particle can be represented as $\Pi(s_i) = \Pi_\Sigma(s_i)\Pi_I(s_i)$, where Π_Σ and Π_I denote the surface and interaction contributions to the rate $\Pi(s_i)$, respectively. In general, the surface rate can be regarded as being proportional to the surface area of particles. Then, the surface contribution to the effective rate $\Pi(s_i)$ can approximately be expressed as $\Pi_\Sigma(s_i) \sim s_i^\beta$ with the exponent $\beta \geqslant 0$ being independent of s_i. Obviously, the underlying scaling relations between surface areas of various objects and their sizes may not exactly be satisfied, especially for small sizes of the objects. Nevertheless, one can easily verify that $0 < \beta < 2/3$ for the case of particles with fractal-like surfaces, while $\beta = 0, 1/2, 2/3$ for 1D, 2D, 3D non-fractal (compact) particles, respectively. For example, $\beta = 0$ in the case of rod like particles that attach molecules at their ends. It should be noted that the exponent β can be found both experimentally and theoretically by determining the surface area and/or mass dimensions of particles.[40,49,50] The interaction part of the effective attachment rate is related to the number, $G(s_i)$, of collisions of the ith molecule (of the size s_i) with a given particle, per unit surface area of the particle and per unit time interval, i.e., $\Pi_I(s_i) \sim G(s_i)$. Assuming that particles are fixed in space and that molecules of the medium undergo the Brownian movement, one has[51–54]

$$G(s_i) = \frac{4\pi D n_0}{W(s_i)} \ , \qquad (1)$$

where D is the diffusion constant for the dispersing medium, n_0 denotes the density of molecules of the medium. The stability ratio $W(s_i)$ is determined by interaction between particles and molecules. This ratio can be expressed as[51]

$$W(s_i) = 2\int_2^\infty \exp[V(r; a_i, a_0)/k_B T]\frac{dr}{r^2} \ , \qquad (2)$$

where V represents the energy due to interactions responsible for aggregation.[51,55] The scaled distance r is defined as $r = 2R/(a_i + a_0)$ with R being the distance between centers of a given particle and a molecule, and a_i, a_0 being radii of the particle and the molecule, respectively. Clearly, the radius a_i is related to the particle size s_i. For instance, in the case of spheroidal particles, one has $a_i^3 = a^3 + [a_0(s_i - 1)]^3$, where a is the radius of the preexisting NP. In general, the resulting dependence of Π_I on s_i is determined by the form of interactions governing the aggregation process in particular systems. Note that, according to the Derjaguin-landau-Verwey-Overbeak theory, particle-molecule couplings that yield main contributions to V are the van der Waals and electrostatic double layer interactions.[55] However, to investigate general properties of the studied model, the interaction part of the attaching rate can also be assumed in the power form, i.e., $\Pi_I(s_i) \sim s_i^\gamma$, where the index γ does not depend of the particle size. The effective aggregation rate is then given by $\Pi(s_i) \sim s_i^\alpha$, where $\alpha = \beta + \gamma$. It should be pointed out that this effective rate is consistent with homogenous collision kernels used to describe coalescence and aggregation processes within the framework of the kinetic theory involving the Smoluchowski equation.[32,34,35] The main difference between the Smoluchowski formalism and the considered approach is that that the number of aggregates is treated here as a constant. Essentially, the index γ and hence the index α can take negative values. However, in such cases, molecules of the media are preferentially attached by small particles. Since the aggregation processes are usually associated with the formation of relatively large particles, the investigation of the model systems considered here is restricted to cases when α is non-negative. Additionally, this exponent is taken to be $\alpha \leqslant 2$. Accordingly, the functional form of the attachment rate is assumed here to be

$$\Pi(s_i) = \left(\frac{s_i}{s_{\max}}\right)^\alpha \ , \ i = 1, 2, ..., n \ , \qquad (3)$$

where $0 \leqslant \alpha \leqslant 2$ and $s_{\max}$ is the maximal size of particles at the current stage of the evolution of the system, i.e., $s_{\max} = \max\{s_i\}_{i=1,2,...,n}$. Thus, by virtue of the above definition, $\Pi(s_i)$ takes values from the unit interval $(0, 1]$. This definition is based on the assumption that the number, n, of particles (seeds) is constant in time. Obviously, the number, $\mathcal{N}_u$, of unconnected molecules of the medium decreases as the aggregation process proceeds. Notwithstanding, the SD can reliably be calculated even if $\mathcal{N}_u$ is assumed to be constant, provided that $\mathcal{N}_u \gg n$.[51] Alternatively, the attachment rate might be determined as being normalized. However, this would considerably elongate duration of numerical simulations of the long time behavior of aggregation ensembles. It should be noted that analogous definitions of attachment rate have been shown to be equivalent for evolving networks, in the sense that one obtains the identical distribution of node degrees for both the definitions.[56]

It should be pointed out that the model does not take into account correlations between the growth of particles. Thus, it corresponds to the case when the concentration of NPs is low at every stage of the evolution of the system, i.e., when the number of unconnected molecules of the media is much larger than the number of particles. Obviously, the algorithm can easily be modified to reflect the aggregation process more precisely. In particular, the attachment rate can be generalized to include the disaggregation by assuming that the size s_i can randomly decrease by one with a rate, different, in general, from the aggregation rate. Although the model involves only one control parameter (the index α), it is shown below to be capable of recovering kinetic behaviors of the most real NP systems.

Numerical analysis of the aggregation kinetics presented below refers to an initial ensemble of n preformed NPs (with sizes $s_i = 1$, $i = 1, 2, ..., n$, and with $s_{\max} = 1$). At each time

step, the algorithm for simulating the growth process of particles runs though the following stages:

(1) A particle, say i, is randomly chosen from the ensemble of n particles.

(2) The size s_i of the randomly chosen particle is increased by one (i.e., a single molecule is attached to the selected particle) with the likelihood determined by the effective attachment rate $\Pi(s_i)$.

(3) In the case when $s_i > s_{\max}$ (after accomplishing the second stage of the aggregation algorithm), the maximal particle size $s_{\max}$ is magnified by one.

To select the particle at random (stage (1)) and to determine the likelihood of connecting a new molecule (stage (2)), the random number generator involving the shuffled nested Weyl sequences[57] is applied, assuming the same starting point for each of the simulated particle ensembles. The calculation procedure is repeated until the total number of attached molecules reaches the value $\mathcal{N} = n \times \overline{N}$, where $\overline{N}$ is the average number of the molecules connected to a preformed NP. Next, the SD is determined by registering numbers $N(s)$ of particles of sizes $s = 1, 2, ..., s_{\max}$, where $s_{\max}$ denotes the maximal particle size of the ultimate ensemble. Note that, since $\overline{N}$ uniformly grows as successive molecules are attached to particles, this quantity can be interpreted as the time of evolution of the system. (Such interpretation of $\overline{N}$ would be rather questionable in case when particles could joint together, as in this case $\overline{N}$ would non-uniformly grow.)

3 Results and discussion

In order to apply the above model for investigating the kinetic behavior of inhomogeneous systems, especially systems with very large particles, the SD of particles have been determined for relatively large total number $\mathcal{N}$ of attached molecules. Generally, the number of preformed NPs has been taken to be $n = 10^5$, while the average numbers of connected molecules has been assumed to be $\overline{N} = 10^3$. Additionally, the dependence of the particle SD on $\overline{N}$ has also been investigated within the range $10 \leqslant \overline{N} \leqslant 2 \times 10^3$. This dependence can be considered as the discrete time evolution of the particle SD. Clearly, the $\overline{N}$-variability of SD appropriately characterizes the evolution of particle ensembles generated by the aggregation algorithm, although the discrete $\overline{N}$-variability of the model ensembles does not precisely match the continuous time evolution of real systems. The behavior of the particle size distribution $N(s)$, determined by counting the number of particles for each particle size $1 \leqslant s \leqslant s_{\max}$, is illustrated in Figs. 1 and 2 for values of the exponent α selected from the range $0 \leqslant \alpha \leqslant 1$. The graphs plotted for $\alpha > 0$ reflect the inhomogeneity of the size of particles evolving under the preferential

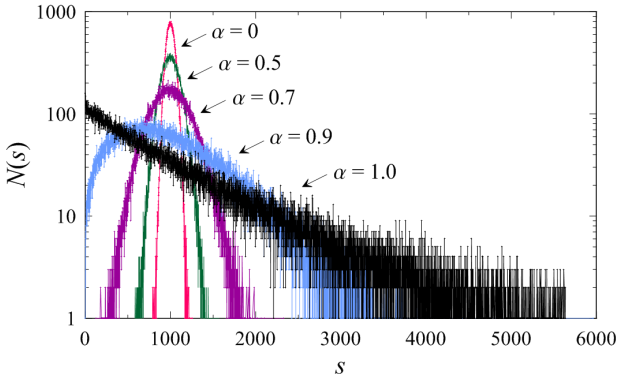

Fig. 1 Semi-log plots of the particle size distribution obtained for $n = 10^5$, $\overline{N} = 10^3$, and for several values of the exponent α. Continuous lines are used for a better visualization.

attachment of molecules. For $\alpha = 0$, the system should essentially be homogeneous and, thereby, the SD should bears a strong resemblance to the Dirac delta function. However, as can be seen from Fig. 1, the SD obtained for $\alpha = 0$ displays a narrow peaked shape and, thereby, has not strictly the form of the Dirac's function. Obviously, this is a consequence of the finiteness of the system and numerical imperfections. A characteristic feature of SD obtained for relatively small values of α, more precisely, for $0 < \alpha < 1$, is the systematic broadening of the peak and the increase in right skewness of the shape as α grows. It is also evident that the SD exhibits an exponential decay at $\alpha = 1$ and that the SD has not a single-peaked form with a maximum at $s > 1$ when $\alpha > 1$ (Fig. 2). In general, the particle SD becomes very irregular for $\alpha > 1$, displaying the scale-free property for relatively small particles, revealing the multimode form for intermediate values of s, and exhibiting right long tail behavior at isolated values of the particle size.

It is remarkable that the model under study here does not predict the lognormal SD. Such a distribution have experimentally been found in various polydispersive systems.[58–60] The

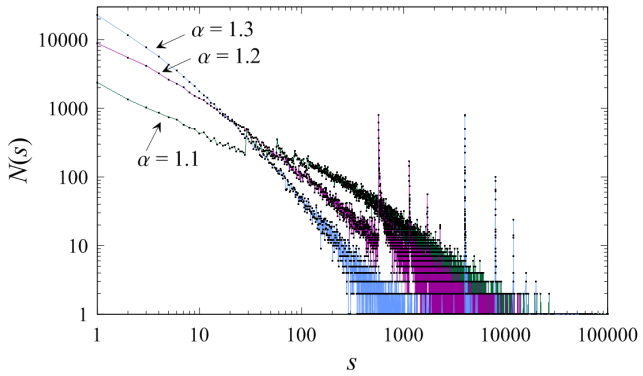

Fig. 2 Continuation of diagrams shown in Fig. 1 for greater values of α: 1.1, 1.2, 1.3. The log-log scale is used.

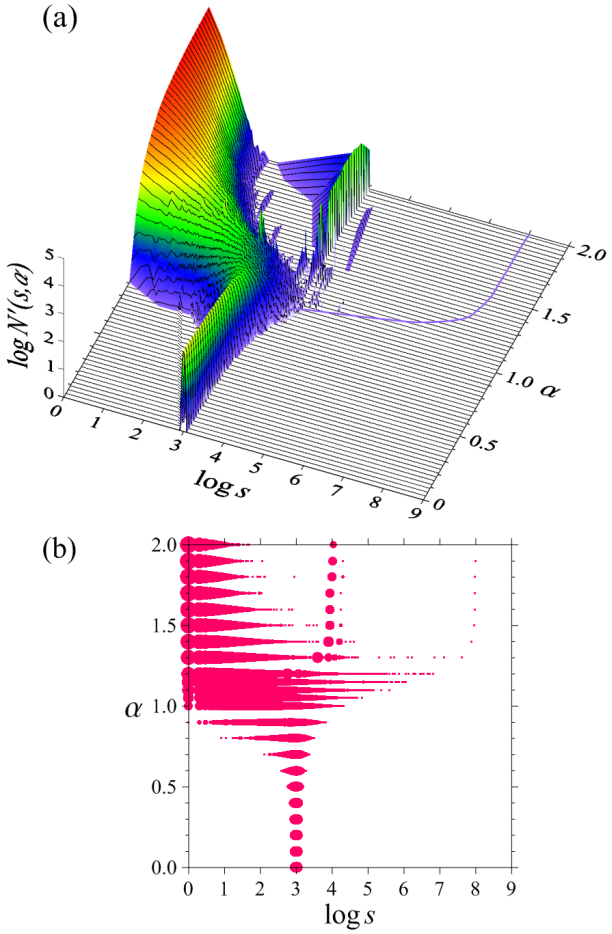

Fig. 3 Particle size distribution as a function of s and α, determined for $n = 10^5$, and $\overline{N} = 10^3$. (a) 3D surface plot, (b) inhomogeneously scaled post map, where points at which $N(s,\alpha)$ is nonzero are represented by filled circles of diameters proportional to $\log N(s,\alpha)$.

lognormal form of the SD has been explained by means of numerical simulations, using the assumptions that the increase of the volume of each particle is proportional to its surface and that the time of particle residence in the growth zone is lognormally distributed in consequence of the diffusion and strong drift.[61] Since the second assumption is not satisfied within the framework of the described model (with the preference rate (3)), the model cannot yield the lognormal SD for any value of the index α.

To gain a more detailed insight into the size dispersion of the model system studied here, the particle SD has been presented as a function, $N'(s,\alpha)$, of both α and s (Fig. 3). Since the surface diagram (Fig. 3a) has been obtained by using inaccurate (by necessity) gridding and interpolation methods, this diagram does not represent the function $N'(s,\alpha)$ quite correctly in some variable regions. Therefore, the function $N'(s,\alpha)$ has additionally been mapped onto the $\log s, \alpha$ plane. Points of the resulting discrete map represent values of variables for which $N'(s,\alpha) > 0$. In order to reflect the variability of $N'(s,\alpha)$ in this map, circles of diameters proportional to $\log N'(s,\alpha)$ have been ascribed to points of the map (Fig. 3b). The results, graphically shown in Fig. 3, evidently indicate that the range of particle sizes grows as α increases. Accordingly, the maximal size $s_{\max}$ is an increasing function of α, displaying a rapid growth as α exceeds the value 1 (Fig. 4). This corresponds to the gelling phenomenon or to the "winner-takes-all" effect occurring when almost all particles do not attach any molecule and, simultaneously, one particle connects enormously many molecules.[32] However, even if α is rather large, say $\alpha > 1.3$, there exist distinctly isolated values and/or ranges of s for which $N'(s,\alpha) > 1$. The regions of s for which the SD takes zero and nonzero values are distinctly separated from each other. Such a multimode behavior of the SD is a consequence of a specific aggregation process occurring in the model systems under discussion here. Indeed, in these systems, particles do not join together and all particles that attached molecules at early stages of the evolution of the resulting particle ensemble remain unchanged or evolve into greater particles. However, due to the inhomogeneity (size dependence) of the aggregation rate, the growth of larger particles is faster than the growth of smaller objects. Then, the combination of evolutionary rules that forbid particles from linking together and that allow particles to connect molecules in a preferential way with respect to the particle size leads, for $\alpha > 1$, to the appearance of multimode behavior of the SD. It is remarkable that the modes of SD are completely separated for sufficiently large α, i.e., regions of s in which they appear do not overlap each other.

The multimodal behavior of SD have been found experimentally in various NP systems. A spectacular example of a very complex multimode SD of real NP systems is given by the SD determined in the case of aggregates created as a result

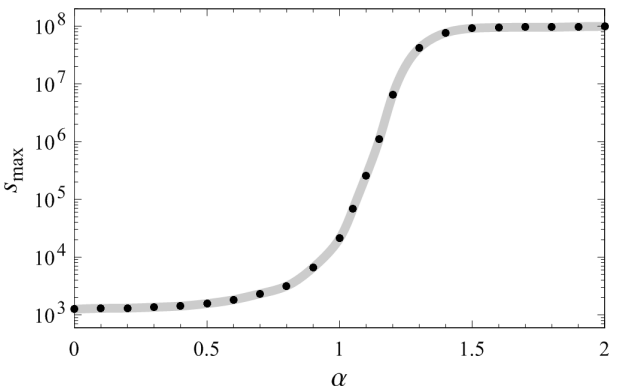

Fig. 4 The maximal particle size as a function of the index α. This dependence has been derived for $n = 10^5$, $\overline{N} = 10^3$, and discrete values of α (marked with dots).

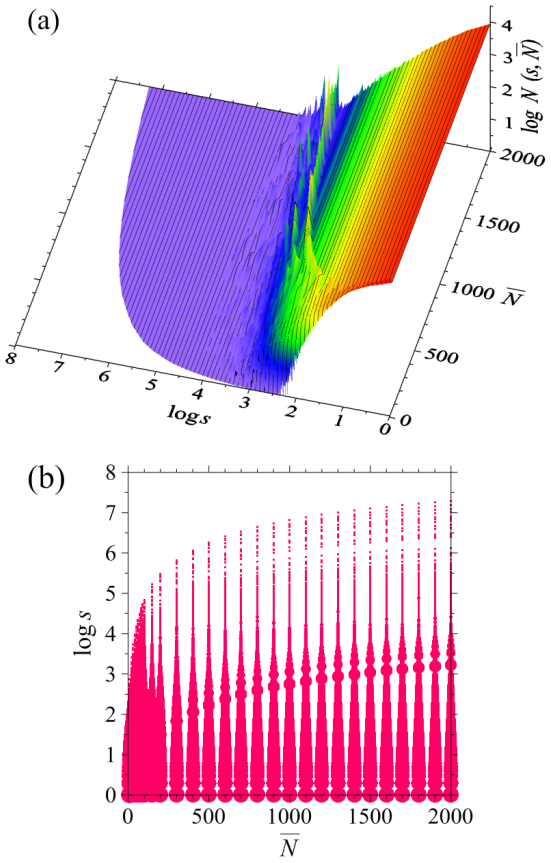

Fig. 5 Dependence of the size distribution $N(s,\overline{N})$ on the particle size and time (represented by the average number $\overline{N}$ of molecules linked to a particle) as obtained for $n = 10^5$ and $\alpha = 1.2$. (a) 3D surface plot, (b) inhomogeneously scaled post map, where circles correspond to values of s and $\overline{N}$ at which $N(s,\overline{N}) > 0$.

of heterogeneous nucleation of polyaniline particles on surfaces of large particles, preformed due to homogeneous nucleation.[20] The process of the heterogeneous nucleation can be described by applying the model considered in this paper. Obviously, mechanisms underlying multimodal SDs determined for various real NP systems can have more complex character than the mechanism considered within the studied model.[20,24] Nevertheless, this model is capable of yielding an adequate description of various nontrivial aggregation structures and, consequently, can be considered as a starting point for describing realistic complex NP systems.

In consequence of the size dependence of the attachment rate, specific dispersion properties of evolving particles become observable when the evolutionary process is continued sufficiently long, i.e., when the average particle size becomes large enough. Clearly, the corresponding temporal evolution of the SD is dependent on α. For $\alpha > 1$, the time variability of the SD turns out to be very complicated. This is illustrated in Fig. 5, where the distribution of particle sizes, $N(s,\overline{N})$, is plotted for $\alpha = 1.2$, as a function of s and time, represented by the average number $\overline{N}$ of molecules linked to a particle. The plots in Fig. 5 indicate that the evolution of small particles, especially those having the size $s = 1$, is relatively slow, whereas the process of evolution of large particles is very rapid. It is obvious that small particles are allowed to attach molecules at each stage of the evolution process, but the growth of large particles, especially the increase of the largest particle, proceeds faster and faster for each $\alpha > 1$, according to the particle size. However, the time dependence of SD is not, in general, monotonously increasing for a given s, as seen in Fig. 5. Indeed, positions of peaks, approximately occurring between $s = 10^2$ and $s = 10^4$, shift in the direction of increasing s as $\overline{N}$ grows. Consequently, the distribution $N(s,\overline{N})$ primarily increases and after a while decreases (for a given $10^2 \leqslant s \leqslant 10^4$). This illustrates a more general property of particle ensembles generated by attaching molecules according to the preferential rate with $\alpha > 1$, i.e., the nonmonotonicity of the time dependence of the SD appearing for each $\alpha > 1$, at some fixed s and, simultaneously, the monotonicity at other values of s. Thus, when $\alpha > 1$, the s and $\overline{N}$ dependence of $N(s,\overline{N})$ does not factorize for all s. This property is in contrast with the typical factorization features of the cluster size distribution determined by using the coagulation Smoluchowski equation with homogeneous kernels (collision rates) involving nonnegative exponents.[32] It should, however, be pointed out that although the ratio $N(s,\overline{N})/N(1,\overline{N})$ depends, in general, on time for fixed $1 < s \ll s_{\max}$, it remains time independent, or nearly time independent, for sufficiently large s and $\overline{N}$ (provided that $\alpha > 1$). Indeed, the evolution of the smallest particles is enormously slowed down for large $\overline{N}$ and then $N(s,\overline{N})$ is approximately constant in time. Simultaneously, the evolution of very large particles (appearing at large $\overline{N}$), especially the evolution of the largest particles, is fast, but the large particles are unique and hence $N(s,\overline{N}) = 1$ for sufficiently large s (as seen in Fig. 5). Since the largest particle connects almost all molecules for $\alpha > 1$ and $\overline{N} \gg 1$, one can expect that, if $\alpha > 1$ and $\overline{N} \gg 1$, the maximal particle size $s_{\max}$ grows linearly with $\overline{N}$. The appropriate time evolution of $s_{\max}$ is graphically presented in Fig. 6 for different values of α. It is seen that $s_{\max}$ can really be expressed in the linear form for large enough $\overline{N}$, such that $\overline{N} > 10^3$, even if α is slightly less than one. More precisely, one then has $s_{\max} \approx c_\alpha \overline{N}$, where the coefficient c_α satisfies the inequality $c_{\alpha'} > c_\alpha$ for $\alpha' > \alpha$. It is remarkable that, within the range of intermediate values of $\overline{N}$, say $10^2 \leqslant \overline{N} \leqslant 10^3$, the time evolution of SD varies in a rather irregular way as α changes. For a given α, the time dependence of $s_{\max}$ is visibly nonlinear in the intermediate range of $\overline{N}$. This follows from the fact that, when $\overline{N}$ is rather small, the maximal particles are too small in order to dominate the aggregation process, and there ex-

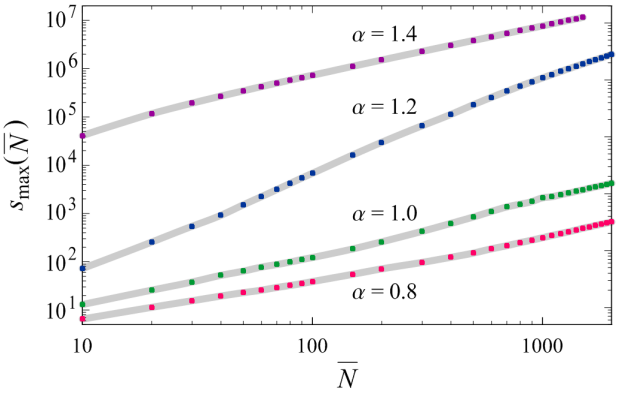

Fig. 6 Time dependence of the maximal size of $n = 10^5$ particles as derived for different values of the index α (time is represented by $\overline{N}$).

ist relatively many smaller particles that, however, undergo a quite fast growth process. As $\overline{N}$ increases, the evolution of aggregates smaller than the largest particle gradually become slower, while the growth of the largest particle is increasingly faster. As a result, SD changes its shape as the evolution of the system progresses.

Since s_{max} rapidly increases as α exceeds the value $\alpha = 1$ (Fig. 4), the rate of attaching a molecule to a small particle tends to zero as $\overline{N}$ increases and then small particles stabilize. On the other hand, the rate of attaching a molecule to the largest particle is equal to one and, for $\alpha > 1$, the largest particle grows linearly with $\overline{N}$. In the case of particles of intermediate sizes, their growth (for $\alpha > 1$) is relatively fast at early evolution stages, but becomes very slow at late stages (Figs. 4 and 5), unexpectedly leading to a multimodal behavior of the SD. As is seen in Fig. 5, the respective peaks of the SD shift toward greater values of the particle size, but heights of the peaks remain nearly unchanged. It must be stressed that the appearance of peaks of the SD at special particle sizes is rather difficult to explain. Beside the multi-peak character of the SD, the multimodality manifest itself in vanishing of the SD function within some ranges of the particle size (Fig. 3). For α greater than $\alpha \approx 1.3$, the intervals within which the SD vanishes appear in regions of both large and relatively small values of the particle size.

An irregular time variability of the shape of the SD has also been recorded experimentally in various NP systems evolving in consequence of aggregation processes.[18,20,24] It is remarkable that, although the detailed mechanisms underlying such a behavior of the SD is, in general, determined by specific properties of individual systems, the complex time variability of the SD can be reproduced within the considered general model (for $\alpha > 1$). This is because the model reflects the competition between largest and smaller real particles in attaching molecules. Moreover, the interparticle interactions occurring in real system depend, in principle, on the size of particles. Obviously, an important role in the evolution of the studied model of NP ensembles plays the constraint that the number of particles is constant. Even though this restriction cannot be satisfied in many real systems, the model can also be useful for studying some systems that evolve in consequence of the particle-particle aggregation and that are close to the liquid-gel phase transition. In such real systems, the average concentration of large particles is usually low and, then, the formation of connections between large particles is unlikely. Instead, large particles frequently attach small particles, analogously to the process of attaching molecules by particles considered within the studied model. Thus, this model can also be applied to describe particle-particle aggregation in strongly inhomogeneous systems at late stages of their time evolution. For instance, in the case of $\alpha > 1$, the model predicts the formation of large particles and simultaneous stabilization of small particles. In some sense, such a process is similar to the Ostwald ripening phenomenon.[62] Since this phenomenon is associated with a continuous dissolution of small particles and, in consequence, with the ultimate disappearance of small particles, the resulting stable SD has a monomodal shape.[62–64] Usually, the underlying mechanism of the dissolution and the size coarsening due to the redeposition of the dissolved species onto large particles is described by assuming that the interfacial tension is constant in time. However, if particle surface areas increase and surfactants stabilizing the particles do not desorb, the surface tension of the molecules varies (in this case, the particle surface is called to be elastic).[65] For relatively low surface elasticity, numerical simulations have shown that the SD evolves over time toward a stable bimodal distribution (with a nonzero minimal particle size).[65] This indicates that, if the dissolution of small particles with elastic surfaces runs faster than the growth of large particles, the total number of particles formed at late stages of the ripening process can be considered to be constant. In such cases, the ripening process can be described by applying the model of preferential attachment of molecules.

4 Conclusions

The simple kinetic model considered in this paper can essentially be applied to analyze the process of the attachment of molecules of liquid media to dispersed NPs. This model involves only one control parameter, i.e., the exponent characterizing the aggregation rate and, therefore, cannot precisely describe various complex aggregation processes occurring in various real systems. However, the model can easily be extended or modified, e.g., by allowing dispersed particles to connect not only molecules of media but also other particles, or by refining the aggregation rate. It is rather evident that a potentially precise theoretical recovery of properties real ag-

gregate ensembles, in particular the recovery the SD of aggregates, can enable a better understanding of complex aggregation processes. This can also give the opportunity to elaborate effective methods to produce aggregation systems of desirable features.

References

1 A.D.Q. Li, *Molecular Self-Assembly: Advances and Applications*, Pan Stanford Publishing, Singapore, 2013.

2 A.C. Balazs, T. Emrick and Th.P. Russell, *Science*, 2006, **314**, 1107-1110.

3 F. Huang, B. Gilbert, H. Zhang nad J.F. Banfield, *Phys. Rev. Lett.*, 2004, **92**, 155501.

4 A.M. Kalsin, A.O. Pinchuk, S.K. Smolukov, M. Paszewski, G.C. Schatz and B. Grzybowski, *Nano Lett.*, 2006, **4**, 1896-1903.

5 S.P. Shields, V. N. Richards and W.E. Buhro, *Chem. Mat.*, 2010, **22**, 3212-3225.

6 H.H. Liu, S. Surawanvijit, R. Rallo, G. Orkoulas and Y. Cohen, *Environ. Sci. Technol.*, 2011, **45**, 9284-9292.

7 H.-G. Liao, L. Cui, S. Whitelam and H. Zheng, *Science*, 2012, **336**, 1011-1014.

8 D. Li, M.H. Nielsen, J.R.I. Lee, C. Frandsen, J.F. Banfield and J.J. De Yoreo, *Science*, 2012, **336**, 1014-1018.

9 T.J. Woehl, J.E. Evans, I. Arslan, W. Ristenpart and N.D. Browning, *ACS Nano*, 2012, **6**, 8599-8610.

10 Y. Liu, X.-M. Lin, Y. Sun and T. Rajh, *J. Amer. Chem. Soc*, 2013, **135**, 3764-3767.

11 D. Zhang, Y. Jiang, X. Wen and L. Zhang, *Soft Matter*, 2013, **9**, 1789-1797.

12 M.L. Eggersdorfer and S.E. Pratsinis, *AICHE J.*, 2013, **59**, 1118-1126.

13 G. Inci, A. Arnold, A. Kronenburg and R. Weeber, *Aerosol Sci. Technol.*, 2014, **48**, 842-852.

14 T.J. Woehl, C. Park, J.E. Evans, I. Arslan, W. Ristenpart and N.D. Browning, *Nano Lett.*, 2014, **14**, 372-378.

15 R.J.J. Williams, C.E. Hoppe, I.A. Zucchi, H.E. Romero, I.E. dell'Erba, M.L. Gómez, J. Puig and A.B. Leonardi, *J. Colloid Interface Sci.*, 2014, **431**, 223-232.

16 T. Kato, *Science*, 2002, **295**, 2414-2418.

17 H.K. Bisoyi and S. Kumar, *Chem. Soc. Rev.*, 2010, **40**, 306-319.

18 T. Gillich, C. Acikgöz, L. Isa, A.D. Schlüter, N.D. Spencer and M. Textor *ACS Nano*, 2013, **7**, 316-329.

19 M. Twomey, Y. Na, Z. Roche, E. Mendes, N. Panday, J. He and J.H. Moon *Macromolecules*, 2013, **46**, 6374-6378.

20 D. Li and R.B. Kaner, *J. Amer. Chem. Soc.*, 2006, **128**, 968-975.

21 B. Gilbert, R.K. Ono, K.A. Ching and C.S. Kim, *J. Colloid Interface Sci.*, 2009, **339**, 285-295.

22 G.M. Whitesides and B. Grzybowski, *Science*, 2002, **295**, 2418-2421.

23 C. Vauthier, B. Cabane and D. Labarre, *Eur. J. of Pharmaceutics and Biopharmaceutics*, 2008, **69**, 466-475.

24 S. Du, K, Kendall, P. Toloueinia, Y. Mehrabadi, G. Gupta and J. Newton, *J. Nanopart. Res.* , 2012, **14**, 475.

25 J.F.A. de Oliveira and M.B. Cardoso, *Langmuir*, 2014, **30**,4879-4886.

26 C. Caumont-Prim, J. Yon, A. Coppalle, F.-X. Ouf and K.F. Ren, *J. Quant. Spectrosc. Radiat. Transfer*, 2013, **126**, 140-149.

27 M.L. Eggersdorfer, D. Kadau, H.J. Herrmann and S.E. Pratsinis, *Langmuir*, 2011, **27**, 6358-6367.

28 M.M. Maye and C.-J. Zhong, *J. Mater. Chem.*, 2000, **10**, 1895-1901.

29 C.B. McKitterick, N.L. Erb-Satullo, N.D. LaRacuente, A.J. Dickinson and P.J. Collings, *J. Phys. Chem. B*, 2010, **114**, 1888-1896.

30 M.R. Tomasik and P.J. Collings, *J. Phys. Chem. B*, 2008, **112**, 9883-9889.

31 R.M. Ziff and E.D. McGrady, *J. Phys. Chem.*, 1985, **82**, 5269-5274.

32 P.G.J. van Dongen and M.H. Ernst, *Phys. Rev. Lett.*, 1985, **54**, 1396-1399.

33 A. Fernández-Barbero, M. Cabrerizo-Vílchez, R. Martínez-Garciá and R. Hidalgo-Álvarez, *Phys. Rev. E*, 1996, **53**, 4981-4989.

34 P.L. Krapivsky and E. Ben-Naim, *J. Phys. A: Math. Gen.*, 2000, **33**, 5465-5475.

35 F. Leyvraz, *Phys. Rep.*, 2003, **383**, 95-212.

36 J.A.D. Wattis, *Physica D*, 2006, **222**, 1-20.

37 C. Connaughton and J. Harris, *J. Stat. Mech.*, 2014, **10**, P05003+19.

38 P. Meakin and F. Family, *Phys. Rev. A*, 1987, **36**, 5498-5501.

39 P. Meakin and F. Family, *Phys. Rev. A*, 1988, **38**, 2110-2123.

40 P. Meakin and M. Muthukumar, *J. Chem. Phys.*, 1989, **91**, 3212-3221.

41 S. di Stasio, A.G. Konstandopoulos and M. Kostoglou, *J. Colloid Interface Sci.*, 2001, **247**, 33-46.

42 H.H. Liu, S.Surawanvijit, R. Rallo, G. Orkoulas and Y. Cohen, *Envir. Sci. Technol.*, 2011, **45**, 9284-9292.

43 I. Kryven, S. Lazzari and G. Storti, *Macromol. Theor. Simul.*, 2014, **23**, 170-181.

44 M.M. Maye, W. Zheng, F.L. Lebowitz, N.K. Ly and C.-J. Zhong, *Langumir*, 2000, **16**, 490-497.

45 Z. Niu and Y. Li, *Chem. Mat.*, 2014, **26**, 72-83.

46 X. Yao, D. Chen and M. Jiang, *J. Phys. Chem. B*, 2004, **108**, 5225-5229.

47 J. Bowers, C.P. Butts, P.J. Martin, M.C. Vergara-Gutierez and R.K. Heenan, *Langmuir*, 2004, **20**, 2191-2198.

48 E. Karatairi, B. Rožič, Z. Kutnjak, V. Tzizios, G. Nounesis, G. Cordoyiannis, L. Thoen, C. Glorieux and S. Kralj, *Phys. Rev. E*, 2010, **81**, 041703+1-5.

49 Y.G. Perez, S.G.F. Leite and M.A.Z. Coelho, *Braz. J. Chem. Eng.*, 2006, **23**, 319-330.

50 Z. Peng, E. Doroodchi, M. Sathe, J.B. Joshi and G.M. Evans, *Adv. Powder Technol.*, 2014, in press.

51 E.J.W. Wervey and J.Th.G. Overbeek, *Theory of the Stabiblity of Lyophobic Colloids*, Elsevier, Amsterdam, 1948.

52 K. Lee, A.N. Sathyagal and A.V. McCormick, *Colloids Surf.*, 1998, **144**, 115-125.

53 T. Kim, K. Lee, M.-s. Gong and S.-W. Joo, *Langmuir*, 2005, **21**, 9524-9528.

54 T. Kim, C.-H. Lee, S.-W. Joo and K. Lee, *J. Colloid Interface Sci.*, 2008, **318**, 258-243.

55 E.M. Hotze, T. Phenrat and G.V. Lowry, *J. Environ. Quality*, 2010, **39**, 1909-1924.

56 W. Jeżewski, *Physica A*, 2005, **354**, 672-680.

57 B.L. Holian, O.E. Percus, T.T. Warnock and P.A. Whitlock, *Phys. Rev. E*, 1994, **50**, 1607-1615.

58 L.E. Wagner and D. Ding, *Transactions ASAE*, 1994, **37**, 815-821.

59 J. Söderlund, L.B. Kiss, G.A, Niklasson and C.G. Granqvist, *Phys. Rev. Lett.*, 1998, **80**, 2386-2388.

60 G. Beaucage, H.K. Kammler and S.E. Pratsinis, *J. Appl. Cryst.*, 2004, **37**, 523-535.

61 L.B. Kiss, J. Söderlund, G.A, Niklasson and C.G. Granqvist, *Nanotechnology*, 1999, **10**, 25-38.

62 A. Baldan, *J. Mat. Sci.*, 2002, **37**, 2171-2202.

63 J.H. Yao, K.R. Elder, H. Guo and M. Grant, *Phys. Rev. B*, 1993, 14110-14125.

64 A. Lazaro, M.C. van de Griend, H.J.H. Brouwers and J.W. Geus, *Micropor. Mesopor. Mat.*, 2013, **181**, 254-261.

65 M.B.J. Meinders, W. Kloek and T. van Vliet, *Langmuir*, 2001, **17**, 3923-3929.